INSTABILITY AND FRONTAL BREAKUP IN SUPER-MENISCUS FILMS

DAWN E. KATAOKA and SANDRA M. TROIAN
Department of Chemical Engineering, Princeton University, Princeton NJ 08544-5263

ABSTRACT

Surface tension gradients created by a nonuniform temperature distribution in a thin liquid film can force vertical spreading beyond the equilibrium meniscus [1]. Experiments designed to probe the flow behavior of super-meniscus films have shown that the leading edge can either spread uniformly with complete surface coverage or become corrugated and breakup into long slender rivulets. We show that within linear stability analysis, both the conditions for unstable flow and the most unstable wavelength compare favorably with recent experiments reported in the literature.

INTRODUCTION

Coating processes usually require a forcing mechanism to induce spreading over the surface. Although flows can be driven by a mechanism as simple as tilting or spinning, flows driven by surface tension gradients have the advantages of operating independent of geometry and allowing the substrate to remain stationary.

Temperature gradient driven films of silicon oils on both vertical [2] and horizontal [3] silicon wafers have been shown to spread with a corrugated leading edge. Such unstable flows exhibit a capillary ridge or "bump" at the leading edge. Surprisingly, similar experiments examining the flow of squalane on a vertical silver plate demonstrate that the film climbs with a uniformly straight front [1]. Furthermore, rather than exhibiting the characteristic advancing ridge, these profiles decrease monotonically as the contact line is approached. The two observations seem contradictory: one would expect similar behavior for both liquid-on-solid systems since the liquids completely wet the different substrates.

It has been proposed in the literature [4] that the capillary ridge must be present in order for the instability to occur. We present here a linear stability analysis of films driven by a constant temperature gradient. This analysis indicates a strong correlation between the presence of a capillary ridge in the unperturbed film thickness profiles and the subsequent formation of long rivulets at the advancing front.

PROBLEM FORMULATION

Governing Equations

Lubrication theory is valid for low Reynolds number flows for which the characteristic extent in the direction of flow is much larger than the film thickness. The temperature gradient driven films observed in Refs. [1–3] are therefore governed by the lubrication equations,

$$\eta \frac{\partial^2 u}{\partial z^2} = \frac{\partial p}{\partial x} + \rho g \tag{1}$$

$$\eta \frac{\partial^2 v}{\partial z^2} = \frac{\partial p}{\partial y} \tag{2}$$

Mat. Res. Soc. Symp. Proc. Vol. 464 © 1997 Materials Research Society

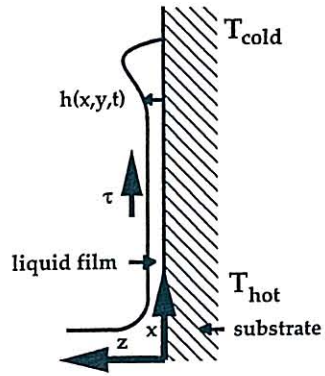

Figure 1: Coordinate system. The y axis points into the page.

$$\frac{\partial p}{\partial z} = 0, \tag{3}$$

where the x axis is along the vertical flow direction, the y axis is in the transverse flow direction, and the z axis is perpendicular to the surface, as illustrated in Fig. (1). The velocity components u and v represent flow in the x and y directions, while p denotes the local pressure in the fluid. The air-liquid interface is described by $z = h(x,y,t)$, which represents the film thickness resting above the stationary substrate located at $z = 0$. The viscosity, density, and local surface tension of the liquid are given by η, ρ, and γ. In the derivation which follows we assume that the temperature distribution mostly affects the local surface tension, with local viscosity or density undergoing smaller changes which are neglected. The boundary conditions are the no-slip requirement at the solid surface

$$u, v|_{z=0} = 0, \tag{4}$$

and constant shear stress at the air-liquid interface

$$\eta \left.\frac{\partial u}{\partial z}\right|_{z=h} = \tau. \tag{5}$$

In regions of the flow where curvature terms become important, we assume relatively small slopes, so that the capillary pressure throughout the film is given by $p = -\gamma \nabla^2 h$. Solving for the height-averaged velocities with contributions from Marangoni flow, capillarity and gravity yields

$$U(x) = \frac{\tau h}{2\eta} + \frac{\gamma}{3\eta} h^2 \nabla \cdot \nabla^2 h - \frac{\rho g h^2}{3\eta} \tag{6}$$

$$V(x) = \frac{\gamma}{3\eta} h^2 \nabla \cdot \nabla^2 h. \tag{7}$$

Substitution of the velocities into the continuity equation

$$\frac{\partial h}{\partial t} + \frac{\partial}{\partial x}(hU) + \frac{\partial}{\partial y}(hV) = 0, \tag{8}$$

with the requirement that the leading edge match smoothly onto a prewetting layer located beyond the nominal contact line gives the film height profiles. For horizontal films, the last term in Eqn. (6) is deleted. Moreover, for vertical geometries, this term can be neglected for sufficiently thin films for which the Marangoni driving force is much larger than drainage by gravity, i.e.

$$h \ll \frac{3\tau}{2\rho g}. \tag{9}$$

Scaling

Away from the leading edge, the film is relatively flat and curvature effects can be neglected. Balancing viscous and Marangoni forces in this "outer" region yields the characteristic velocity scale for the system

$$U_c = \frac{\tau h}{2\eta}. \tag{10}$$

Near the spreading front, curvature effects must be included; the interface must curve in order to contact the substrate. Inclusion of capillary effects in the balance with viscous and Marangoni forces gives the characteristic length scale over which the interface curvature is significant

$$l = h_c(3Ca)^{-\frac{1}{3}}, \tag{11}$$

where Ca is the capillary number, defined by

$$Ca = \frac{\eta U_c}{\gamma}, \tag{12}$$

and h_c represents the film thickness at the leading edge of the outer region.

To address the stability of the leading edge which occurs in the vicinity of the capillary region, we must first solve for the unperturbed film thickness profiles in the inner region. We therefore rescale all variables in a manner similar to other driven flow problems [4–6]. This rescaling effectively stretches the appropriate variables in such a way as to balance contributions among all the local forces present in the capillary region. Spatial coordinates are rescaled by l, the film thickness h by h_c, and time by U_c/l. Rescaling of Eqn. (8) yields the appropriate dimensionless evolution equation for the film thickness

$$\hat{h}_{\hat{t}} + (1+b)\hat{h}_{\xi} - \frac{\partial}{\partial\xi}\left[\hat{h}^2 - \hat{h}^3(\hat{h}_{\xi\xi\xi} + \hat{h}_{\xi\zeta\zeta})\right] + \frac{\partial}{\partial\zeta}\left[\hat{h}^3(\hat{h}_{\zeta\xi\xi} + \hat{h}_{\zeta\zeta\zeta})\right] = 0. \tag{13}$$

The solution to (13) must satisfy the two required boundary conditions in ξ,

$$\hat{h} \to 1 \quad as \quad \xi \to \infty \tag{14}$$

$$\hat{h} \to b \quad as \quad \xi \to -\infty. \tag{15}$$

A third boundary condition in ξ is unnecessary; Eqn. (13) lacks explicit ξ dependence and is therefore translationally invariant. Boundary conditions in ζ and an initial condition in $\hat{t}$ are also not needed since the form of the profile disturbance in ζ and $\hat{t}$ will be specified. The

variables ξ and ζ are the dimensionless x and y coordinates, and $\hat{h}$ and $\hat{t}$ are the dimensionless film thickness and time. The ξ coordinate has been scaled such that the origin translates with the contact line so that ξ is positive in the upstream direction. The parameter b is the ratio of the precursor film thickness to the characteristic film thickness h_c.

RESULTS

Base Flow

To solve for the base flow profile and perturbation, we expand the film thickness as

$$h(\xi,\zeta,t) = h_0(\xi) + \epsilon h_1(\xi,\zeta,t), \tag{16}$$

where h_0 denotes the unperturbed film profile, h_1 is the disturbance, and ϵ is a small parameter representing the strength of the applied perturbation. (The hats have been dropped for clarity.) We find the shape of the unperturbed film and the perturbation by substituting the expanded form of h into Eqn. (13). The base flow is given by the $O(1)$ equation

$$h_{0\xi\xi\xi} = \frac{1}{h_0} - (1+b)\frac{1}{h_0^2} + b\frac{1}{h_0^3}, \tag{17}$$

which must satisfy the boundary conditions

$$h_0 \to 1 \quad as \quad \xi \to \infty \tag{18}$$

$$h_0 \to b \quad as \quad \xi \to -\infty. \tag{19}$$

Again, a third boundary condition is unnecessary because (17) is translationally invariant. Numerical solutions to (17) for various precursor thicknesses are plotted in Fig. (2). Note that the height of the capillary ridge decreases with an increase in the precursor layer thickness.

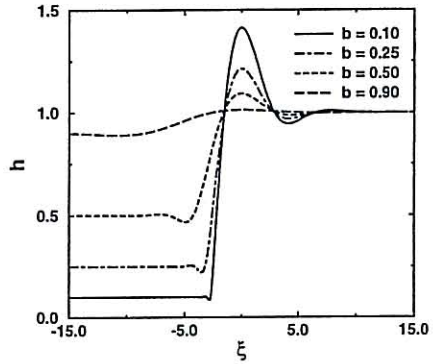

Figure 2: Base flow film profiles for various prewetting layer thicknesses. The profiles have been shifted to align the profile maxima.

Linear Stability Analysis

The shape of the disturbance is given by keeping the $O(\epsilon)$ terms and substituting in the normal mode form for the disturbance

$$h_1(\xi,\zeta,t) = G(\xi)exp(iq\zeta + \beta t), \tag{20}$$

where q denotes the wavenumber of the disturbance in the transverse flow direction and β is the eigenvalue or growth rate of the perturbation. The resulting linear equation

$$\beta G + (1+b)G_\xi - \frac{\partial}{\partial\xi}\left[2Gh_0 - 3Gh_0^2 h_{0\xi\xi\xi} - h_0^3\left(G_{\xi\xi\xi} - q^2 G_\xi\right)\right] + h_0^3\left(q^4 G - q^2 G_{\xi\xi}\right) = 0 \tag{21}$$

is subject to decay boundary conditions

$$G, G_\xi \to 0 \quad as \quad \xi \to \infty \tag{22}$$

$$G, G_\xi \to 0 \quad as \quad \xi \to -\infty. \tag{23}$$

Numerical solutions to Eqn. (21) for the largest growth rate as a function of wavenumber are illustrated in Fig. (3). Note that the magnitude of the disturbance growth rate decreases with an increase in the precursor film thickness.

DISCUSSION AND CONCLUSIONS

The above theoretical analysis is valid for constant shear stress driven flows for which gravity is negligible. The base flow profiles of these spreading films contain a capillary ridge at the leading edge whose magnitude decreases with an increase in the prewetting layer thickness (Fig. 2). As the capillary ridge decreases or as the precursor layer increases, the flow becomes more stable. As illustrated in Fig. (3), the film becomes marginally stable for a prewetting layer thickness that is about half as thick as the characteristic thickness of the spreading film. This result indicates a strong correlation between the capillary ridge thickness and the linear stability of the film.

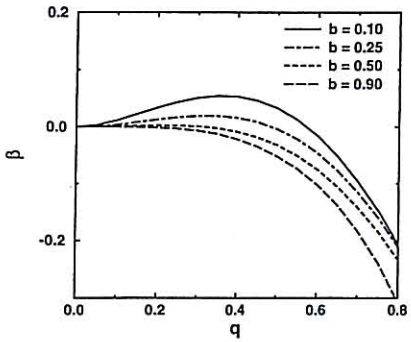

Figure 3: Dispersion relationship illustrating the largest eigenvalue β as a function of wavenumber q for the films illustrated in Fig. (2).

We have compared our predictions with experiments reported in the literature for spreading silicon oil films [2,3]. The climbing films were sufficiently thin to satisfy Eqn. (9), and horizontal films were unaffected by drainage. The theoretical analysis assumes, however, the presence of a prewetted layer ahead of the leading edge. Although the surfaces were not precoated in the experiments, evaporation/condensation, van der Waals forces, or diffusion may have deposited a very thin layer of fluid ahead of the spreading front. The presence of such a prewetting layer was found by Carles et al [7]. It appears therefore that the theoretical predictions for very small prewetting layers most closely resembles the experimental conditions. Small values of b yield relatively large capillary ridge thicknesses, which are in agreement with experimental observations. Furthermore, the observed instability is consistent with the theoretical prediction that flow with large capillary ridges become unstable. In addition, we have found that the most unstable wavelength is $\lambda \approx 18l$, which is in excellent agreement with experiments [8].

In contrast to the silicon oil films, the squalane films reported in Ref. [1] lacked a capillary ridge and spread with a straight front. The small temperature gradients used in these experiments produced films of sufficient thickness for which drainage velocities become comparable to Marangoni velocities. Inclusion of drainage by gravity in the theory is expected to eliminate the capillary ridge to produce theoretical profiles which decrease monotonically as the edge is approached. We are currently investigating the stability of Marangoni driven flows with the inclusion of drainage. If the additional mechanism eliminates the bump and suppresses the instability, this result will provide strong evidence for the link between the presence of the bump and the instability and will elucidate the reason behind the discrepancy between the similar experimental systems.

ACKNOWLEDGMENTS

This material is based upon work supported under an NSF Graduate Fellowship (DEK) and an NSF Research Initiation Award through Grant No. CTS-9409579 (SMT).

REFERENCES

1. V. Ludviksson and E.N. Lightfoot, AIChE J. **17**, p. 1166 (1971).

2. A.M. Cazabat, F. Heslot, S.M. Troian, and P. Carles, Nature **346**, p. 824 (1990).

3. J.B. Brzoska, F. Brochard-Wyart, and F. Rondelez, Europhys. Lett. **19**, p. 2 (1992).

4. S.M. Troian, E. Herbolzheimer, S.A. Safran, and J.F. Joanny, Europhys. Lett. **10**, p. 25 (1989).

5. J.A. Moriarty, L. Schwartz, and E.O. Tuck, Phys. Fluids **3**, p. 733 (1991).

6. M.A. Spaid and G.M. Homsy, Phys. Fluids **8**, p. 460 (1996).

7. P. Carles, A.M. Cazabat, and E. Kolb, Colloids and Surfaces A **79**, p. 65 (1993).

8. D.E. Kataoka and S.M. Troian, submitted to J. Colloid Interface Sci.